Fatigue life sensitivity of monopile-supported offshore wind turbines to damping

Ramtin Rezaei[a], Paul Fromme[b], Philippe Duffour[a]

[a]Department of Civil, Environmental & Geomatic Engineering, UCL, London, WC1E 6BT, UK

[b]Department of Mechanical Engineering, UCL, London, WC1E 6BT, UK

Contact Author: p.fromme@ucl.ac.uk

Abstract

Offshore wind energy is an important renewable electricity source in the UK and Europe. Monopiles are currently the most commonly used substructures to support offshore wind turbines. The fatigue life of offshore wind turbines is directly linked to the oscillatory bending stresses caused by wind and wave loading. The dynamic response of the structure is highly dependent on the combined aerodynamic, hydrodynamic, structural, and soil damping present. The fatigue life sensitivity of a reference 5MW wind turbine under operational and non-operational conditions has been investigated using time-domain finite element simulations. The model uses beam elements for the monopile and tower and includes nonlinear p-y curves for soil-structure interaction. The effects of the wind turbine operation, environmental loads, and variable damping levels on the fatigue life were investigated systematically. The fatigue life increases significantly as a result of reductions in the bending stress caused by increased damping. From a practical point of view, significant cost-savings could be achieved in the design of a wind turbine by fitting supplemental damping devices. An efficient approximate method is proposed to assess the influence of damping, by scaling the vibration amplitudes around the first natural frequency of the system.

Keywords: Offshore wind turbine; Fatigue life calculation; Vibration analysis; Renewable energy

1 Introduction

Offshore wind electricity generation has become one of the fastest growing renewable energy technologies. Europe has focused extensively on the development of offshore wind energy, to the extent that almost 90% of the largest offshore wind farms in the world are located there [1,2]. Monopiles are currently the most common type of support structure for offshore wind turbines. The fatigue life of offshore wind turbines (OWT) is directly linked to the stress induced by the structural vibrations due to environmental (wind and wave) loading. As a dynamic system, the magnitude of the response of an OWT depends on the amplitude of the applied forces, the proximity of the natural frequencies to the dominant forcing frequencies and the damping. As wind turbines are lightly damped structures, a good estimate of the damping is crucial to predicting their dynamic response accurately. The overall damping in offshore wind turbines is mostly comprised of aerodynamic, hydrodynamic, structural and soil damping, and damping due to supplemental damping devices such as tuned-mass dampers. There is significant uncertainty about each of these contributions. Soil damping depends on the soil type and is particularly difficult to measure directly. Different values for soil damping ratios in offshore wind turbines mounted on monopiles have been suggested in literature [3-6], varying from 0.17% [4] up to 1.3% of critical damping [6]. Aerodynamic damping is the highest contributor to the overall damping, but it mostly acts in the fore-aft direction when the turbine is in operation. In parked conditions, good agreement is found for the side-side and fore-aft damping levels reported in literature [7–9]. In this case, the overall damping is reported to be about 1% of critical damping in the fore-aft direction and 1.5% for the side-side mode. In the operational range, the aerodynamic damping is known to be variable and the levels proposed in the literature vary from 2% to 8%, depending on the wind speed, size and operation of the wind turbine [10–12].

Offshore wind turbines are generally designed for a minimum of 20 years of service life [13] and the predicted fatigue life of the system has to match this [14,15]. Four methods of fatigue assessment for structures are commonly used; simplified method, spectral method, time-domain method and deterministic method [16]. As the aerodynamic loading has a wide bandwidth, damage calculation methods in the frequency domain lead to very conservative estimates [17]. Time-domain approaches are considered the most reliable for the prediction of fatigue life as nonlinear and stochastic load effects caused by the environmental loads and soil-structure interaction can be taken into account [18]. In addition, various hybrid frequency/time-domain fatigue analysis methods have been proposed [17–21], typically using transfer functions to obtain the response in the frequency-domain [17,18,22–25]. However, in general predictions of fatigue life are considered less accurate than using time-domain methods.

The influence of damping on the fatigue damage of offshore wind turbines has been mostly considered in parked/non-operational conditions in the literature. The fatigue assessment of OWT is usually carried out by simulating and analysing the stress at critical locations such as the tower base [25, 26] or the mudline [27]. The effect of damping in a parked condition was studied and it was demonstrated that the maximum bending moment could increase by 20% as a result of a 50% change in damping [6]. It was further shown that the mudline bending moment during an extreme wind and wave event is decreased by 5% if damping is increased by 1% [4]. The effect of soil damping has been studied and up to 47% reduction in fatigue damage due to a 4% increase in soil damping has been reported [26]. It was also suggested that a complete lifetime simulation including damping effects could clarify the influence on the fatigue life of OWTs, which has not been reported in literature.

This paper investigates systematically the effects of damping on the fatigue life of offshore wind turbines. The study is based on time-domain finite element (FE) simulations carried out on a reference offshore wind turbine supported by a monopile, including soil-structure interaction. The fatigue life was calculated by adding the damage contributions from representative environmental states in the operational wind speed range. The methodology is described in section 2. Section 3 discusses the relevant features of the wind and wave loads. In section 4, the effects of variable damping and operational state (shutdowns) are studied systematically. The contribution of increased damping on increased fatigue life is investigated. A novel approximate method is proposed, significantly reducing the computational costs associated with time-domain simulations for multiple damping levels (requiring only one full time-domain analysis for one level of damping with little additional computational effort for other damping levels), while allowing accurate predictions of the effect of increased damping on prolonged fatigue life.

2 Methodology

2.1 Modelling approach

As fatigue affects mostly structural details (e.g. welds), it must be assessed using a comprehensive and realistic structural model. Following other researchers [26, 28–31], this study is based on a reference 5MW case study wind turbine model mounted on a monopile, for which the US National Renewable Energy Laboratory (NREL) has provided a significant amount of data [32]. According to initial design reports [33], it was due to be constructed at a location approximately 10 km off the Dutch coast in the North Sea. The complete fatigue analysis was carried out in different stages using a combination of software packages. The process is shown schematically in Fig. 1. The wave and wind loads were calculated based on available meteorological data for the proposed site. Wave load time-series were obtained in MATLAB by inverse-Fourier Transform of the JONSWAP spectrum [34]. Wind load time histories were calculated using FAST, a software package provided by NREL, which includes a validated model of the turbine chosen here. FAST simulates an incoming turbulent wind field (TurbSim module) and then computes the aerodynamic interaction of the flow with the blades using Blade Element Momentum theory. FAST also provides an estimate of the aerodynamic damping, which is otherwise difficult to obtain. As FAST has limited capabilities for modelling soil-structure interaction and only allows for a basic structural model of the tower/monopile, the wind loads obtained from FAST and wave loads from Matlab were used as input to an FE model (ABAQUS) of the OWT which comprised the tower, monopile and soil system. Response stress time histories were computed and recorded in ABAQUS at critical locations for various load time series.

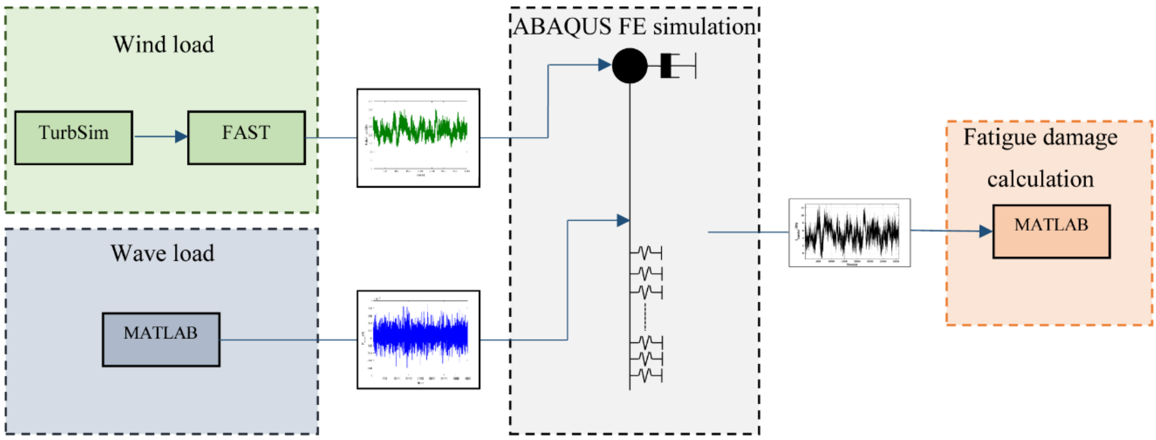

Figure 1. Schematic of simulation software packages for fatigue life calculation.

2.2 Geometry and properties of the OWT and monopile

The reference wind turbine is a 3-bladed wind turbine, shown schematically in Fig. 2 with key dimensions. The rotor diameter is 126m, and the hub height at 92m above mean sea level. The monopile embedded depth is 45m for a water depth of 21m. The NREL 5MW wind turbine uses a Repower 5M machine. The rotor blades are based on a LM-Glasfiber Holland design with a length of 62.7m [35]. A slight modification to the blades adopted here was suggested in reference [32], which truncated the length of the blades by 1.1m to be similar to those suggested for the Repower 5M machine. The operational range of wind speeds for this turbine is between 3m/s to 25m/s, with the rated rotor speed at 12.1 rpm.

The pile has a 6m diameter with a constant thickness, while the tower has a tapered section with the diameter decreasing linearly from 6m at the bottom to 3.87m at the top (Fig. 2). In this study, the thickness of the pile and tower sections were modified from the original documents [32] to ensure that the natural frequency of the wind turbine lies between the 1P (rotor) and 3P (blade passing) frequencies with a margin of 10%. A pile thickness of 80mm and linearly varying tower thickness of 28-38mm were used to ensure that the first natural frequency of the system lies at 0.25Hz.

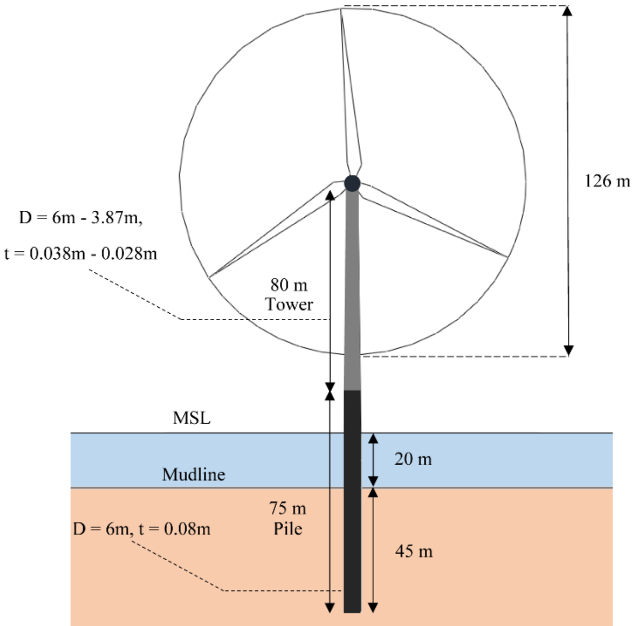

Figure 2. Reference 5MW wind turbine dimensions.

The steel used for the monopile is assumed to have an elastic modulus of 210GPa, a Poisson ratio of 0.3 and a density of 7850 kg/m^3. A higher density steel (ρ=8500kg/m^3) was used for the tower section to take into account the added mass of secondary steel [32].

2.3 Numerical simulation

The OWT time response due to the combined non-periodic aerodynamic and wave loading was simulated using the FE software ABAQUS. The equation of motion of the structure was implicitly solved for small amplitude vibrations. The FE Model comprises the tower and monopile, modelled using linear Timoshenko beam elements (ABAQUS: B21 element). The rotor was modelled as a lumped mass located at the top of the tower. The soil-structure interaction was modelled with nonlinear horizontal springs (p-y curves) connecting the monopile to a fixed reference (see section 2.4). A preliminary study showed that 0.5m length elements produced sufficiently converged results, with less than 0.5% change in the results when the element size was reduced from 1m in length. Good agreement with relevant reports on the 5MW NREL wind turbine was obtained [32]. The dynamic analysis for fatigue calculations was done using implicit simulations with time increments of 0.1s. Following recommended practice, a one-hour simulation length was used throughout this paper. A preliminary study of fatigue damage sensitivity to simulation time confirmed that this was acceptable. Four hundred seconds were added at the start of the load time series and the corresponding simulation data was later discarded to avoid any potential initial transient effects. Numerical damping is normally applied by default in ABAQUS to stabilise the numerical scheme. This was set to zero as damping is a key factor for this study that needs to be controlled carefully. The stabilisation of the solution was achieved by applying damping in the model. Offshore wind turbines can be considered as lightly damped structures (overall damping ratios typically lower than 10% of critical damping). Therefore, the energy dissipation processes can be linearized, with the amplitude of dynamic response only depending on the correct overall amount of damping. The model accuracy was checked for different implementations of the damping (e.g. Rayleigh & dashpot damping), and the same response was obtained for the same overall damping ratio. The structural, hydrodynamic and soil damping were combined and modelled as Rayleigh damping, which is common practice [7, 11, 26]. The aerodynamic damping was simulated through a dashpot at the top of the monopile in the direction of the wind load [36]. This provides a spatial distribution closer to the real system and allows this damping contribution to be varied independently. The Rayleigh damping was kept constant throughout as 2% of critical damping, incorporating structural (1%), hydrodynamic (0.2%) and soil (0.8%) damping contributions based on literature [3, 6]. The aerodynamic damping was varied independently from 4% to 9% based on literature values [10], as described in the following sections.

2.4 Soil structure interaction modelling

In the FE model, the bottom of the monopile was supported vertically on a roller while 30 horizontal springs were distributed every 1.5m along the embedded height of the pile to model the lateral soil-structure interaction. Following DNV [14] and API [37], non-linear p-y curves were used to define the stiffness of the springs following the soil properties listed in Table 1. P-y curves are further described in references [38, 39] for homogeneous and layered soils. For the actual loads in an offshore wind turbine, most of the soil-structure interaction occurs on the initial, linear part of the p-y curves. This has been employed for the approximate method (section 4.4), which effectively linearizes the soil-structure interaction. Due to the lack of data for the planned location, the soil profile used here was based on an interpolation of available data from neighbouring sites whose soil profile mostly consists of medium-dense to dense sand, as used in reference [40].

Table 1. Soil profile for proposed location, modified according to data from [40]. γ_{sat} is the saturated unit weight, and ϕ' is the angle of friction of the soil layers.

Soil layer	Layer description	γ_{sat} (kN/m^3)	ϕ'
0m to -15m	Loose sand	17	27.5
-15m to -20m	Firm clay	19	20
-20m to -25m	Fine to medium sand	19	32.5
-25m to -65m	Fine to medium sand	19	35

2.5 Environmental load calculation

Aerodynamic and hydrodynamic loads are the driving dynamic forces in the fatigue of offshore wind turbines. The relative directionality of wave and wind loads has been the subject of research [6]. For this study, the wind and wave loads are assumed to be in the same direction as a likely worst case scenario. In reference [25], 3D scatter diagrams of wind speed (V_w), significant wave height (H_s) and zero-crossing wave periods (T_z) were used to create a set of environmental states, which were applied in this research. Wind speeds ranging from 4m/s to 24m/s were grouped into 2m/s bins. Wave heights and periods were grouped in 0.5m and 1s bins, respectively. Environmental states (ES) were defined by correlated wind and wave bins. The environmental states were classified into 22 states as shown in Table 2 [25], in line with other studies that used a similar number of ES [41, 42]. As expected, the ES with higher wind and wave intensities have a significantly lower probability of occurrence, while the majority of ES occur with wave heights of below 2m, wave period of less than 4.5s and wind speeds of less than 15m/s. The operational ES (Table 2) account for 91% of probability of occurrence, with most of the remaining 9% corresponding to wind speeds below the cut-in speed and thus low contribution to fatigue damage.

Table 2. Environmental states, based on data from [25].

State	V_W (m/s)	T_Z (s)	H_S (m)	P_{State} (%)
1	4	3	0.5	3.95
2	4	4	0.5	3.21
3	6	3	0.5	11.17
4	6	4	0.5	7.22
5	8	3	0.5	11.45
6	8	4	1.0	8.68
7	10	3	0.5	5.31
8	10	4	1.0	11.33
9	12	4	1.0	5.86
10	12	4	1.5	6.00
11	14	4	1.5	4.48
12	14	5	2.0	3.26
13	16	4	2.0	1.79
14	16	5	2.5	3.10
15	18	5	2.5	1.74
16	18	5	3.0	0.80
17	20	5	2.5	0.43
18	20	5	3.0	1.14
19	22	5	3.0	0.40
20	22	6	4.0	0.29
21	24	5	3.5	0.15
22	24	6	4.0	0.10

Mann [43] and Kaimal [44] spectra are the main turbulent wind models suggested in practice. In this study, the Kaimal spectrum was used to model the wind turbulence. The wind speeds for the selected ES are all within the operational range of the reference wind turbine. However, in this paper, the turbine will be considered in three possible states: (i) in operation, (ii) stationary and blades feathered (least drag) and (iii) stationary and pitched-out blades (maximum drag). In operation, a constant blade pitch and rotor speed were considered for a given mean wind speed at hub height. The rotor thrust was calculated using FAST by constraining the tower and monopile to be rigid. These thrust time series were then used as the input wind load in ABAQUS. This approach, where the separately calculated wind and wave loads are combined in an FE software, has been used in various references [25,31]. The wind and wave loads were calculated using 0.1s time increments to match the FE time steps.

The random nature of the wave load for the North Sea conditions is most commonly captured through the JONSWAP [34] spectrum, a modified version of the Pierson-Moskovitz (P-M) [45] spectrum. The surface velocities and accelerations were defined according to linear (Airy) wave theory. Wheeler stretching was applied to the velocity and acceleration terms to account for the variation of the mean sea surface. The wave force on the vertical pile was calculated using Morison's equation. The effect of currents on the wave force was considered by adding the mean current velocity to the water particle velocities in the drag component of the wave load, as the current results in a static transverse force on the pile. The resultant hydrodynamic pressure was applied as a point load at the mean sea level.

2.6 Fatigue life calculation

Design guidelines provide a recommended practice for the fatigue life calculation of offshore wind turbines that is followed here. DNV [46] proposes various S-N curves to assess the fatigue capacity of details in offshore structures. S-N curves are defined by Eq. (1), where N refers to the number of cycles to failure, $log(\bar{a})$ corresponds to the intercept of $log\ (N)$ axis, $\Delta\sigma$ is the stress range, m is the negative inverse slope of the curve and SCF is the stress concentration factor. t and t_{ref} are the thickness through which the crack is likely to grow (i.e. thickness of the monopile) and a reference thickness, respectively. In the current study a bi-linear S-N curve class E, which is suggested for piles, is used and the parameters for the considered location of circumferential welding are shown in Table 3.

$$\log(N) = \log(\bar{a}) - m\log((\Delta\,\sigma(SCF))\left(\frac{t}{t_{ref}}\right)^{k}) \qquad (1)$$

Table 3. S-N curves parameters, according to [46].

$\mathbf{N \leq 10^6}$		$\mathbf{N \geq 10^6}$		**Thickness component**	**Hot-spot consideration**
Log($\bar{a}_1$)	m_1	Log($\bar{a}_2$)	m_2	k	SCF
11.61	3.0	15.35	5.0	0.2	1.13

The fatigue damage was calculated at the location of maximum stress at an assumed welding point. The location of maximum stress in the monopile was investigated and it was found to be approximately 8m below the seabed and sensitive to changes in the seabed condition (for instance due to scour).

The random nature of the loading results in variable amplitude stress outputs. Rainflow counting was used to bin the stress amplitudes into multiple stress levels and count the number of cycles in every stress bin. Once the stress output was rainflow-counted, the results were used to find the damage caused by every stress bin and then added together to obtain the total damage in the monopile for a given stress time-history. The damage D in the pile for a given ES j was calculated using the Palmgren-Miner (PM) sum rule as shown in Eq. (2)

$$D_j = \sum_{i=1}^{N_C} \frac{n_i}{N_i} \, , \tag{2}$$

where n_i is the number cycles counted within a given stress bin, N_i is the number of cycles to fatigue failure [47] for the nominal stress cycle amplitude i, and N_C is the total number of bins counted over the one hour time history. Denoting D_{ref}^{1hr} the damage required in one hour of simulation time that would lead to a total damage of 1 (failure according to PM sum rule) over 20 years. D_{ref}^{1hr} is used to normalise the damage calculated for each ES.

As each ES j has a different probability of occurrence p_j, the normalised contribution of ES j to the total fatigue damage is $DC_j = \frac{D_j}{D_{ref}^{1hr}} p_j$ and the total fatigue damage is obtained by summing each damage contribution according to Eq. (3), with $^{20\ years}/_{D}$ the resultant fatigue life of the monopile:

$$D = \sum_{j=1}^{N_j} DC_j \,. \tag{3}$$

Fatigue damage calculation was verified using harmonic loading simulation. The fatigue damage at the mudline was calculated using the rainflow counting and fatigue life calculation MATLAB scripts and compared and verified with the analytically calculated damage. Using this methodology, the fatigue life of the reference turbine system was predicted for various levels of aerodynamic damping and operational regimes.

3 Influence of operational regime on loads

The operational regime of the wind turbine determines the aerodynamic forces and damping on the structure. Figure 3(a) shows the mean resultant wave loads and their standard deviation for the sea states considered. The mean and standard deviation of the aerodynamic and hydrodynamic loads were used to quantify their static and dynamic (varying) components. With increasing wave height and period, the static component of the wave load increases only slightly, whereas the dynamic component increases significantly. Figure 3(b) and (c) show the mean and standard deviation of the operational and non-operational wind loads for each ES. For the non-operational wind turbine, feathered and pitched-out blades are considered separately. As one would expect, the aerodynamic load is significantly higher when the blades are pitched-out than when they are feathered. As the 'intensity' of the ES increases, so do the mean and standard deviation of the rotor thrusts. When the wind turbine is in operation, the mean wind load peaks at the rated wind speed and then decreases (as blades are increasingly feathered), whereas the standard deviation of the load shows a continuous increase with the wind speed due to turbulence. The mean rotor thrust for the operational wind turbine is normally higher than for the non-operational feathered wind turbine. In the case of pitched out blades, the mean wind thrust for very high wind speeds (environmental states 22 and 24) is greater than during operation, where blades are turned out of the wind. Significantly lower load turbulence is present for the non-operational wind turbine compared to that experienced by the pitch-controlled operational wind turbine as the rotor is stationary.

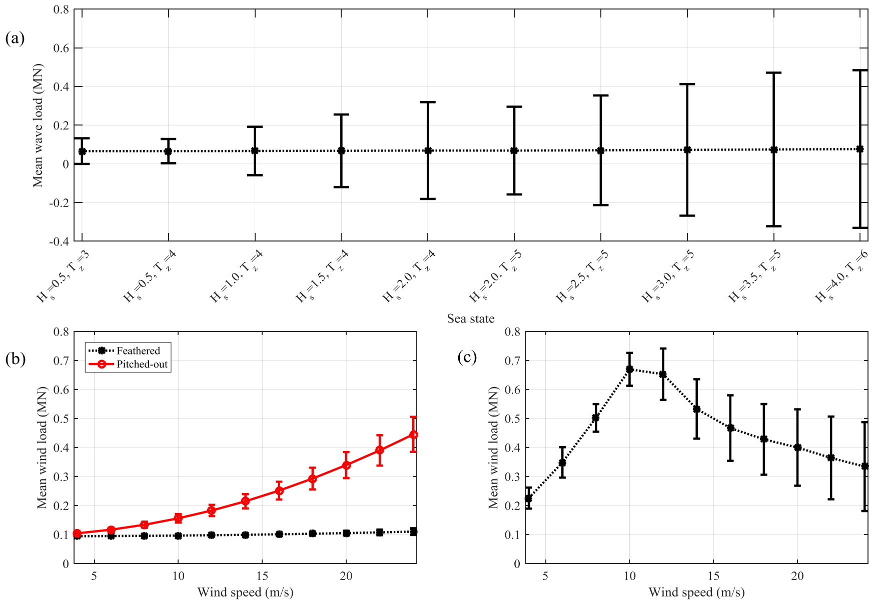

Figure 3. Mean (static component) and standard deviation (variable component) of the environmental loads: (a) wave load; (b) non-operational wind load (feathered and pitched-out); (c) operational wind load.

As a wind turbine is a cantilevered structure, the highest bending moment and stresses occur close to the bottom, with a significantly higher lever arm and thus bending moment contribution from the wind load during operation. Figure 4(a) shows the mean and standard deviation of the mudline bending moment for the non-operational wind turbine, calculated from the combined wind and wave forces. When the blades are feathered, the wind load is approximately constant and the mean and standard deviation of the mudline bending moment is mainly driven by the increase in the variable component of the hydrodynamic loads. However, when the blades are pitched-out, the higher lever arm of the wind thrust leads to an increasing mean mudline bending moment. The standard deviation of the bending moment at mudline increases as both wind and wave loads have increasing dynamic components. Figure 4(b) shows the mean and standard deviation of the mudline bending moment for the operational wind turbine. The mean value peaks at the ES corresponding to the rated wind speed and then slowly decreases, following the wind speed pattern observed in Figure 3(c).

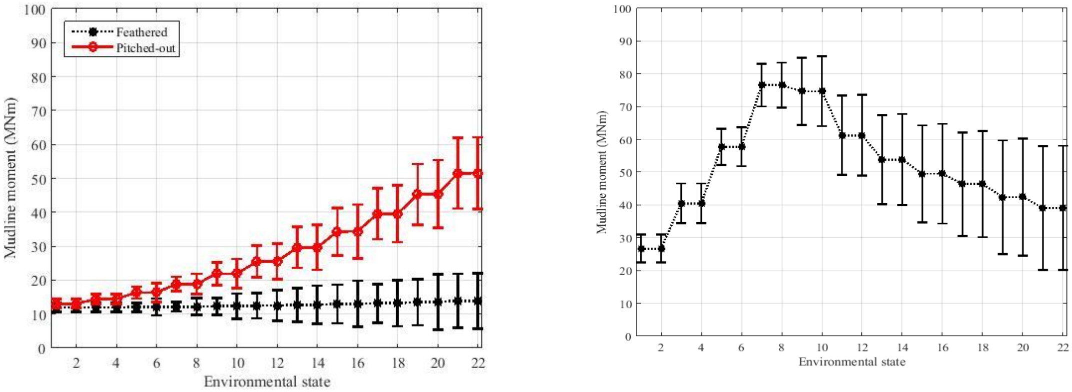

(a) (b)

Figure 4. Mean (static component) and standard deviation (dynamic component) of mudline bending moment for (a) non-operational wind turbine; (b) operational wind turbine.

As the soil stiffness is not infinite, the location of the maximum longitudinal stress in the monopile (relevant for fatigue) is not at the mudline. Figure 5 shows the variation of the bending moment along the depth of the monopile caused by applying 1MN wind and wave loads. For the soil conditions considered, the maximum bending moment in the reference monopile occurs approximately 8m below the mudline. Assuming the maximum stress occurs at the mudline instead of its actual location could result in an error of approximately 15% in the stress amplitudes in the monopile, significantly underestimating fatigue damage. Note that the location of this maximum stress is specific to the geometry considered here and could shift depending on the soil properties, water depth, scour depth and the respective magnitudes of the loads.

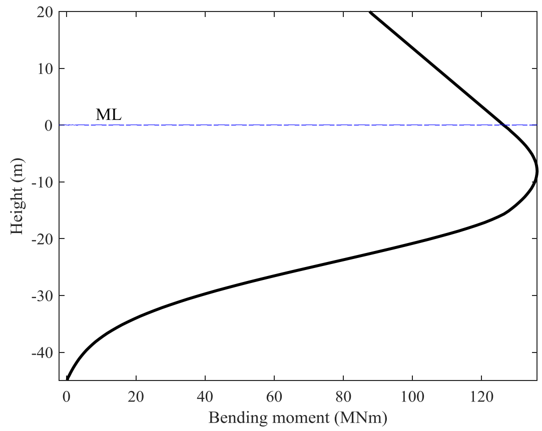

Figure 5. Bending moment in the reference monopile for 1MN wind and wave loads.

4 Fatigue analysis results

4.1 Effect of variable damping

In this section, the effect of the variation of damping with wind speed is investigated by comparing the fatigue life of the OWT when damping is assumed variable or constant. Variable aerodynamic damping values with respect to wind speed were taken from [48], ranging from 3.7% to 5.4% depending on the wind speed (Table 4), with the maximum value close to the rated operational wind speeds. These values are realistic, but only used for illustrative purposes as they are based on a smaller wind turbine. The average value of damping of approximately 4.5% was used as a constant value for comparison.

Table 4. Aerodynamic damping ratio contributions at different wind speeds, based on data from [48].

Wind speed (m/s)	4	6	8	10	12	14	16	18	20	22	24
Aerodynamic damping (%)	4	4	3.7	4.4	4.6	5.4	5.3	4.9	4.7	4.5	4.3

Simulation results (not presented graphically) showed that considering a variable aerodynamic damping had mixed effects on fatigue damage. For ES where the variable damping is appreciably higher than average (e.g. states 11-14), the fatigue damage contribution was reduced by up to 16%. For other ES, the variable damping values are close to the average and the ES probabilities of occurrence are low enough that the effect on fatigue damage contribution was minimal. Overall, the fatigue life was calculated as 31 years for the constant damping case and 33 years for the variable damping case – a 7% increase in the predicted fatigue life of the system. Given that the values of varying aerodynamic damping are difficult to obtain and come with significant uncertainty [48], this rather small difference in fatigue life suggests that in practice assuming a constant aerodynamic damping for all wind speeds leads to acceptable fatigue life estimates. Therefore, a constant aerodynamic damping is assumed throughout the remainder of the paper.

4.2 Operational versus non-operational wind turbine

Although the environmental loads considered are in the operational range of the wind turbine, this section investigates the long-term effects on the fatigue life of wind turbine shut-downs. As they cause both a decrease in load and in damping, their overall effect is difficult to assess without a complete fatigue life calculation. Approximately 5% of aerodynamic damping for the operational wind turbine was suggested in reference [12], and as described in the introduction, structural damping is reported to be approximately 1-2%. Therefore, a reference damping of 2% for the non-operational and 7% for the operational wind turbine was assumed in this section.

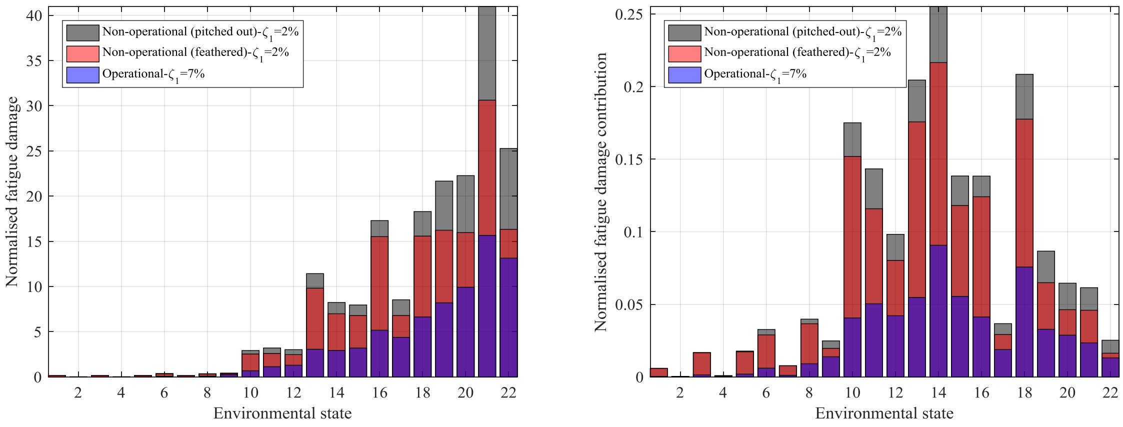

(a) (b)

Figure 6. (a) Normalised damage and; (b) normalised fatigue damage contribution of the environmental states for operational and non-operational (feathered and pitched-out) wind turbines. Bars are overlaid (i.e. all start from zero).

Figure 6(a) shows the normalised damage for each ES, comparing the operational turbine with non-operational (feathered and pitched-out) loads and damping. The environmental loads and resulting bending moments for the operational and non-operational wind turbine can be seen in Figs. 3 and 4. Figure 6(b) shows the contribution of the ES to the fatigue damage of the wind turbine, taking the probability of occurrence of each state (Table 2) into account. Figure 6(a) shows that the fatigue damage increases in general with increasing wind speed and wave height, with slight variations due to the dynamic amplification from the forcing frequencies. The lower ES (up to #8) do not lead to significant fatigue damage. The ES that are above the rated wind speed of the operational wind turbine lead to a significantly higher fatigue damage. This confirms that the wind load has a high contribution to the fatigue damage of operational systems. In non-operational mode, the fatigue damage is dominated by the dynamic wave load. Feathered blades lead to lower damage than pitched-out blades due to the lower aerodynamic load component. Figure 6(a) shows that in spite of the lower aerodynamic loads in the non-operational cases, the fatigue damage is significantly higher due the absence of aerodynamic damping.

Figure 6(b) shows that fatigue life is dominated by the contribution of the ES around the rated wind speed. The predicted fatigue life of the operational wind turbine is approximately 33 years, as opposed to 11 years for the pitched-out and 14 years for the feathered non-operational cases. The importance of the aerodynamic damping is clearly demonstrated by the fact that the higher operational damping compensates for the higher rotor loads and results in a fatigue life that is more than twice the fatigue life of the non-operational case. ES are paired up such that odd-numbered states have the same wind speed as the following even-numbered state, so damage variation within each pair can be attributed only to different wave loading. For instance, in Fig. 6(a) environmental states 21 and 22 have the same wind speed of 24m/s but different wave loads (Table 2). The difference in the fatigue damage of these environmental states are approximately 40% for the non-operational wind turbine, but considerably lower for the operational case. These large variations, due to the differences in wave loading, are a feature characteristic of ES with above-rated wind speed (see also ES 15-16 and 17-18) and can be explained by a combination of the higher magnitude of wave loads and the proximity of the wave peak frequency to the first natural frequency of the wind turbine.

4.3 Damping influence

In this section, a set of damping levels is considered to examine their effect on the fatigue damage in the wind turbine. The levels of damping applied to the operational wind turbine model range from 4% to 11%, including 2% applied in the form of Rayleigh damping to account for structural, hydrodynamic and soil damping. The standard deviation of the longitudinal stress (at 8m below the seabed) shows a reduction of approximately 7%, 13%, and 17% for an increase of 2%, 5%, and 7% in the overall damping of the system. These reductions are higher than those reported in reference [26] in the operational range of the wind turbine (value of the aerodynamic damping not stated).

Figure 7(a) shows the normalised fatigue damage and Fig. 7(b) shows the contribution of the normalised damage of each ES at various damping levels while the turbine is in operation. As expected, the fatigue damage observed with 4% overall damping is the highest. Higher damping levels lead to a reduction in fatigue damage, but the reduction varies to some degree depending on the wind and wave loading for each ES.

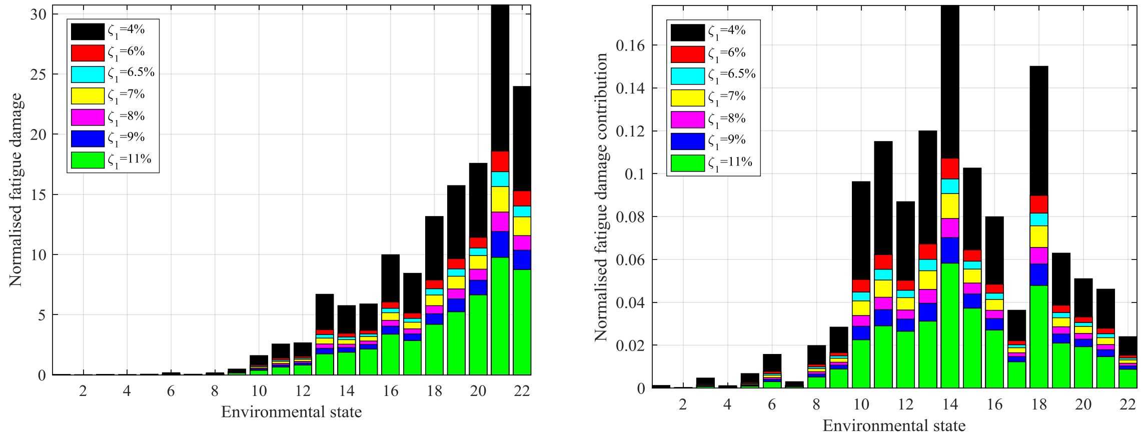

(a) (b)

Figure 7. (a) Fatigue damage, and (b) fatigue damage contribution for every enviromental state at different levels of total damping.

The lower ES show a larger reduction, while the damage reductions for ES above the rated wind speed converge to similar levels. Compared to the values for 4% overall damping, the fatigue damage for 6% total damping reduces by an average of approximately 45%. This decrease is even more pronounced and reaches 75% when 11% total damping is considered. The contribution of an ES to the overall fatigue of the structure depends on the combination of its probability of occurrence and absolute damage. In general, the higher ES have lower probabilities of occurrence but cause more damage. ES 1 to 9 have a low contribution to the fatigue of the system due to their low normalized fatigue damage (Fig. 7(a)). The most damaging environmental states are at and above the rated wind speed, with ES 14 and 18 contributing the most damage due to the combination of normalised fatigue damage and probability of occurrence (Table 2). The combined contribution of fatigue damage from ES 10 to 18 is more than 70% of the overall damage.

Figure 8 shows the projected fatigue life of the wind turbine (100% operational) based on the damage contributions obtained for the different damping values shown in Fig. 7(b). The design fatigue life of 20 years is marked as a reference. An almost linear increase in fatigue life is observed when damping increases, from 16 years at 4% overall damping to 53 years at 11% damping. The changes in the overall fatigue life are consistent with the average reductions in the ES damages as shown in Fig. 7(a) and demonstrate the potential fatigue life extension of a wind turbine structure with additional damping, e.g. in the form of a tuned-mass damper or other structural modifications. Wind turbines are regularly shut down for short maintenance and inspection periods, but breakdowns can lead to longer non-operational periods during operational ES until repairs can be carried out. In a hypothetical scenario where the turbine is left parked for an extended period, the fatigue damage is increased, as was shown in section 4.2 from the comparison of operational and non-operational wind turbines. Assuming respectively 5% and 10% downtime (95% and 90% operational) and summing the proportional damage, a reduction in the fatigue life of the wind turbine of approximately 2% and 4% is predicted, indicating a potential danger of prolonged downtime.

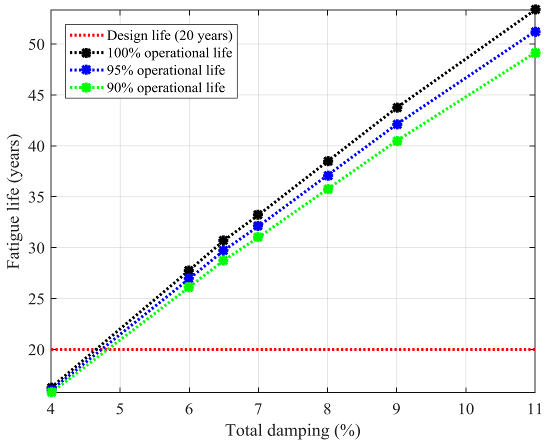

Figure 8. Fatigue life comparison for various levels of damping and operational life.

4.4 Approximate method for the prediction of fatigue life

In this section, a hybrid time-domain approach is proposed, which only requires the full time-domain analysis for one level of damping and uses it to predict the fatigue life at other damping levels with little additional computational effort. The outline of the simplified fatigue analysis is shown in Fig. 9. In this method, the output stresses from the time-domain simulations of a reference damping level are transformed into the frequency-domain. The dynamic amplification factor (DAF) of an equivalent single degree of freedom system (SDoF), which can be easily obtained from the dynamic properties of the wind turbine, is used as a substitute for the transfer function of the FE model. The reference stresses are scaled by the frequency-dependent ratio of amplification of the response between each damping level and the reference. The scaled stresses are then converted back into the time domain and rainflow counted to determine the fatigue damage in the wind turbine structure.

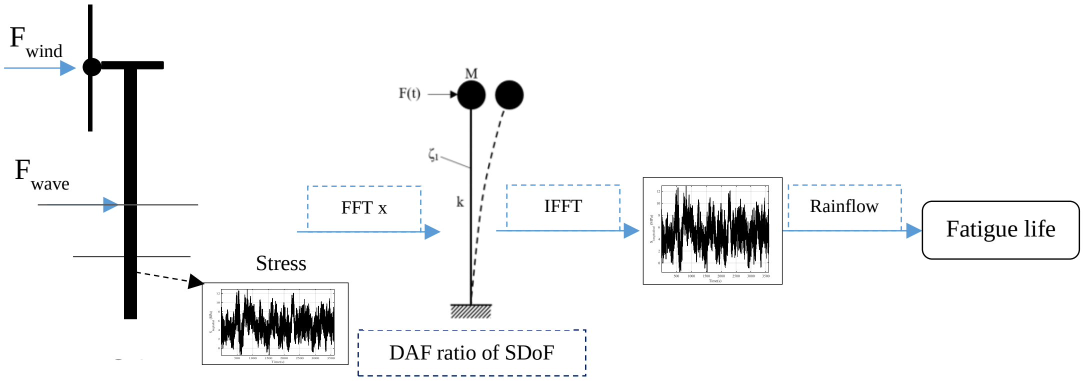

Figure 9. Schematic flow chart of the simplified fatigue analysis method.

The mass of the equivalent single degree of freedom system is the first modal mass (M_1) and the stiffness (k) was chosen so that the first natural frequency of the turbine (0.25 Hz) is identical to that of the SDoF system. The influence of damping was studied by choosing as a reference damping a mid-level value of ζ_1=7% (comprising 5% aerodynamic and 2% structural, soil and hydrodynamic damping). To test the accuracy using the DAF of a SDoF instead of the actual transfer function, a set of idealised harmonic wind and wave loads with identical amplitudes of 0.5MN and frequencies $\Omega_1 = 0.2Hz$, $\Omega_2 = 0.25Hz$ and $\Omega_3 = 0.3Hz$ were applied in the time-domain with different damping levels. Subsequently, the steady-state portions of the maximum longitudinal stress in the monopile at 8m below seabed were compared for each force frequency. The stresses calculated using the DAF were compared to the stress time histories from the full time simulations. A close match was observed, approximately within 1% for almost all damping values tested. Comparison of the fatigue life showed a maximum deviation of 2% between the approximate analysis and full simulations. To test the influence of the reference damping level, an alternative damping level of ζ_1=11% was selected as reference and the comparison of the stress ratios showed approximately 2% deviation. Thus, the selection of reference damping level is considered to have only a minor influence on this analysis.

Actual aerodynamic and hydrodynamic loads are stochastic with broadband frequency content. Using those as input, longitudinal stress time histories at the reference damping of ζ_1=7% were obtained from the FE simulations for each ES, to obtain the fatigue damage. Figure 10 compares the normalised damage contributions calculated using the simplified fatigue analysis with those from the time-domain analysis for the highest damping level of ζ_1=11% (using 7% damping as reference). As can be seen, the normalised damage contributions obtained from the two methods show a close match, with a slight underestimation of the fatigue damage for some ES by up to 2% with the approximate method.

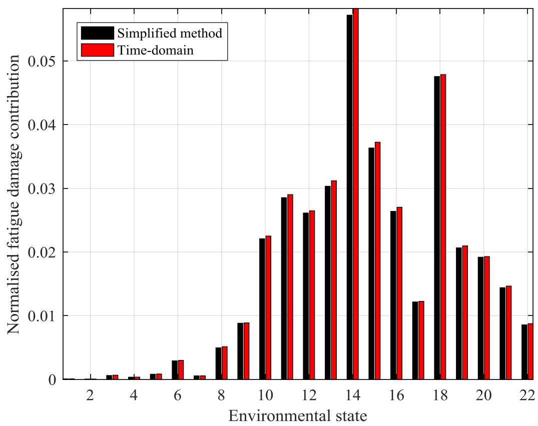

Figure 10. Comparison of the normalised damage contribution in the simplified fatigue analysis method with the time-domain results.

Figure 11 shows the fatigue lives predicted using the simplified method against those predicted using full time-domain simulations. As can be seen, the fatigue life predictions show a very good match with a largest difference of 2% for 11% damping. The hybrid time-domain approach requires only a full time-domain analysis for one level of damping with little additional computational effort, e.g., for the 6 damping levels shown in Fig. 11 the simulation time was reduced by approximately 75%.

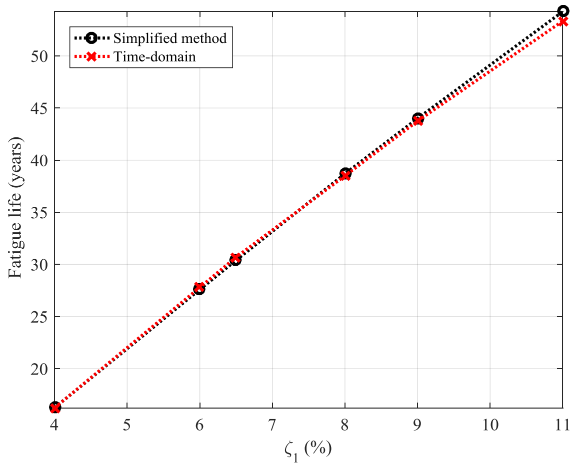

Figure 11. Fatigue life predictions from the simplified and the time-domain fatigue analyses of the wind turbine.

For the loads experienced at this intermediate water depth, the small differences found in the fatigue life prediction show that dynamic amplification factors can be used to quickly assess the influence of damping on the fatigue life of the wind turbine with good accuracy and little extra effort. This can be particularly useful at a preliminary design stage.

5 Conclusions

The effects of damping on the fatigue life of an offshore wind turbine structure were investigated systematically for the detailed FE model of a 5MW case study wind turbine. Fatigue damage is mainly driven by the bending stresses caused by the vibrations due to wind and wave loads. Assuming a constant average aerodynamic damping for all wind speeds was found to lead to accurate fatigue life estimations compared to allowing aerodynamic damping to vary with wind speeds. Normal or unforeseen shutdowns of the wind turbine during operational environmental states can result in increased fatigue damage of up to 60%, as the significant reduction in aerodynamic damping has a larger influence than the reduced loading.

Prolonged maintenance or shut-down periods could reduce the fatigue life to an unsafe level, therefore this scenario should be included as part of the fatigue limit state analysis.

Moderate damping increases were shown to effectively reduce fatigue damage by up to 67%. The predicted fatigue life of offshore wind turbines showed an almost linear increase with the level of damping, from 16 years at 4% overall damping to 53 years at 11% damping. Therefore significant cost-savings could be achieved in OWT design by incorporating damping devices (e.g. tuned-mass-dampers), reducing the levelized electricity costs of the renewable energy system. An approximate hybrid time-domain method was developed, significantly reducing the computation time required to accurately assess the influence of damping on fatigue (requiring only a full time-domain FE analysis for one level of damping with little additional computational effort for other damping levels). In this paper, only unidirectional wind and wave loads were considered. The consideration of the directionality of wave and wind loads and their influence on fatigue life is recommended for further research.

References

[1] J.K. Kaldellis, D. Zafirakis, The wind energy (r)evolution: A short review of a long history, Renew. Energy. 36 (2011) 1887–1901. doi:10.1016/j.renene.2011.01.002.

[2] X. Sun, D. Huang, G. Wu, The current state of offshore wind energy technology development, Energy. 41 (2012) 298–312. doi:10.1016/j.energy.2012.02.054.

[3] N.J. Tarp-Johansen, L. Andersen, E. Christensen, C. Mørch, B. Kallesøe, S. Frandsen, Comparing Sources of Damping of Cross-Wind Motion, in: Proc. Eur. Offshore Wind 2009 Conf. Exhib., The European Wind Energy Association, Stockholm, Sweden, 2009: pp. 1–10.

[4] W. Carswell, J. Johansson, F. Løvholt, S.R. Arwade, C. Madshus, D.J. DeGroot, A.T. Myers, Foundation damping and the dynamics of offshore wind turbine monopiles, Renew. Energy. 80 (2015) 724–736. doi:10.1016/j.renene.2015.02.058.

[5] W. Versteijlen, A. Metrikine, J.S. Hoving, E. Smidt, W.E. De Vries, Estimation of the vibration decrement of an offshore wind turbine support structure caused by its interaction with soil, in: Proc. EWEA Offshore 2011 Conf., European Wind Energy Association, Amsterdam, The Netherlands, 2011.

[6] M. Damgaard, L.V. Andersen, L.B. Ibsen, Dynamic response sensitivity of an offshore wind turbine for varying subsoil conditions, Ocean Eng. 101 (2015) 227–234. doi:10.1016/j.oceaneng.2015.04.039.

[7] R. Shirzadeh, C. Devriendt, M. a. Bidakhvidi, P. Guillaume, Experimental and computational damping estimation of an offshore wind turbine on a monopile foundation, J. Wind Eng. Ind. Aerodyn. 120 (2013) 96–106. doi:10.1016/j.jweia.2013.07.004.

[8] M. El-Kafafy, G. De Sitter, C. Devriendt, W. Weijtjens, Monitoring resonant frequencies and damping values of an offshore wind turbine in parked conditions, IET Renew. Power Gener. 8 (2014) 433–441. doi:10.1049/iet-rpg.2013.0229.

[9] C. Devriendt, P.J. Jordaens, G. De Sitter, P. Guillaume, Damping estimation of an offshore wind turbine on a monopile foundation, in: Proc. EWEA 2012 Conf., Copenhagen, Denmark, 2012.

[10] M.H. Hansen, K. Thomsen, P. Fuglsang, T. Knudsen, Two methods for estimating aeroelastic damping of operational wind turbine modes from experiments, Wind Energy. 9 (2006) 179–191. doi:10.1002/we.187.

[11] C. Koukoura, A. Natarajan, A. Vesth, Identification of support structure damping of a full scale offshore wind turbine in normal operation, Renew. Energy. 81 (2015) 882–895. doi:10.1016/j.renene.2015.03.079.

[12] D.J.C. Salzmann, J. van der Tempel, Aerodynamic damping in the design of support structures for offshore wind turbines, in: Proc. Offshore Wind Energy Conf., Copenhagen, Denmark, 2005: pp. 1–9.

[13] Det Norske Veritas, Support structures for wind turbines (DNVGL-ST-0126), Norway, 2016.

[14] Det Norske Veritas, Design of Offshore Wind Turbine Structures, Norway, 2013.

[15] IEC, Wind Turbines - Part 3: Design requirements for offshore wind turbines, Brussels, Belgium, 2009.

[16] American Bureau of Shipping (ABS), Guide for the fatigue assessment of offshore structures, Houston, TX, USA, 2014.

[17] J. Du, H. Li, M. Zhang, S. Wang, A novel hybrid frequency-time domain method for the fatigue damage assessment of offshore structures, Ocean Eng. 98 (2015) 57–65. doi:10.1016/j.oceaneng.2015.02.004.

[18] Y.M. Low, Extending a time/frequency domain hybrid method for riser fatigue analysis, Appl. Ocean Res. 33 (2011) 79–87. doi:10.1016/j.apor.2011.02.003.

[19] V. Michalopoulos, Simplified fatigue assessment of offshore wind support structures accounting for variations in a farm, Delft University of Technology, 2015.

[20] S.F. Mohammadi, N.S. Galgoul, U. Starossek, P.M. Videiro, An efficient time domain fatigue analysis and its comparison to spectral fatigue assessment for an offshore jacket structure, Mar. Struct. 49 (2016) 97–115. doi:10.1016/j.marstruc.2016.05.003.

[21] B. Yeter, Y. Garbatov, C. Guedes Soares, Evaluation of fatigue damage model predictions for fixed offshore wind turbine support structures, Int. J. Fatigue. 87 (2016) 71–80. doi:10.1016/j.ijfatigue.2016.01.007.

[22] L.S. Etube, Variable Amplitude Corrosion Fatigue and Fracture Mechanics of Weldable High Strength Jack-Up steels, University College London, 1998.

[23] A. Halfpenny, A frequency domain approach for fatigue life estimation from finite element analysis, in: Int. Conf. Damage Assess. Struct. (DAMAS 99), Dublin, 1999.

[24] L.S. Etube, F.P. Brennan, W.D. Dover, Stochastic service load simulation for engineering structures, Proc. R. Soc. A Math. Phys. Eng. Sci. 457 (2001) 1469–1483. doi:10.1098/rspa.2000.0719.

[25] J. van der Tempel, Design of support structure for offshore wind turbines, Delft University of Technology, 2006.

[26] C.M. Fontana, W. Carswell, S.R. Arwade, D.J. DeGroot, A.T. Myers, Sensitivity of the Dynamic Response of Monopile-Supported Offshore Wind Turbines to Structural and Foundation Damping, Wind Eng. 39 (2015) 609–628. doi:10.1260/0309-524X.39.6.609.

[27] E. Marino, A. Giusti, L. Manuel, Offshore wind turbine fatigue loads: The influence of alternative wave modeling for different turbulent and mean winds, Renew. Energy 102 (2017) 157–169. doi:10.1016/j.renene.2016.10.023.

[28] L.I. Lago, F.L. Ponta, A.D. Otero, Analysis of alternative adaptive geometrical configurations for the NREL-5 MW wind turbine blade, Renew. Energy. 59 (2013) 13–22. doi:10.1016/j.renene.2013.03.007.

[29] W. Shi, H.C. Park, C.W. Chung, H.K. Shin, S.H. Kim, S.S. Lee, C.W. Kim, Soil-structure interaction on the response of jacket-type offshore wind turbine, Int. J. Precis. Eng. Manuf. Technol. 2 (2015) 139–148. doi:10.1007/s40684-015-0018-7.

[30] J.P. Blasques, A. Natarajan, Mean load effects on the fatigue life of offshore wind turbine monopile foundations, in: B. Brinkmann, P. Wriggers (Eds.), Comput. Methods Mar. Eng. V - Proc. 5th Int. Conf. Comput. Methods Mar. Eng. Mar. 2013, International Center for Numerical Methods in Engineering (CIMNE), Hamburg, Germany, 2013: pp. 818–829.

[31] N. Alati, V. Nava, G. Failla, F. Arena, A. Santini, On the fatigue behavior of support structures for offshore wind turbines, Wind Struct. 18 (2014) 117–134. doi:10.12989/was.2014.18.2.117.

[32] J. Jonkman, S. Butterfield, W. Musial, G. Scott, Definition of a 5-MW reference wind turbine for offshore system development, Colorado, USA, 2009.

[33] H.J. Kooijman, C. Lindenburg, D. Winkelaar, E.. van der Hooft, DOWEC 6 MW PRE-DESIGN, Aeroelastic modelling of the DOWEC 6 MW pre-design in PHATAS, The Netherlands, 2003.

[34] K. Hasselmann, T.P. Barnett, E. Bouws, H. Carlson, D.E. Cartwright, K. Enke, J.A. Ewing, H. Gienapp, D.E. Hasselmann, P. Kruseman, A. Meerburg, P. Muller, D.J. Olbers, K. Richter, W. Sell, H. Walden, Measurements of Wind-Wave Growth and Swell Decay during the Joint North Sea Wave Project (JONSWAP), Ergnzungsh. Zur Dtsch. Hydrogr. Zeitschrift R. A(8) (1973) 1–95.

[35] C. Lindenburg, Aeroelastic Modelling of the LMH64-5 Blade, The Netherlands, 2002.

[36] S. Schafhirt, M. Muskulus, Decoupled simulations of offshore wind turbines with reduced rotor loads and aerodynamic damping, Wind Energ. Sci. Discuss. (2017), doi:10.5194/wes-2017-29

[37] API (American Petroleum Institute), Recommended Practice for Planning , Designing and Constructing Fixed Offshore Platforms — Working Stress Design, 2007.

[38] J.M. Murchison, M.W. O'Neill, Evaluation of p-y relationships in cohesionless soils, analysis and design of pile foundations, in Proc. Symposium in Conjunction with the ASCE National Convention, Americal Society of Civil Engineers (ASCE) (1984) 174–191.

[39] M. Georgiadis, Development of p-y curves for layered soils, in Proc. Geotechnical Practice Offshore Engineering, New York, USA: Americal Society of Civil Engineers (ASCE) (1983) 536–545.

[40] R.S. Nehal, Foundation Design Monopile 3.6 & 6.0 MW wind turbines, Amstelveen, The Netherlands, 2001.

[41] L. Ziegler, S. Voormeeren, S Schafhirt, M. Muskulus, Design clustering of offshore wind turbines using probabilistic fatigue load estimation, Renew. Energy 91 (2016) 425-431. doi:10.1016/j.renene.2016.01.033.

[42] D. Zwick, M. Muskulus, Simplified fatigue load assessment in offshore wind turbine structural analysis, Wind Energy 19 (2016) 265-278. doi:10.1002/we.1831.

[43] J. Mann, The spatial structure of neutral atmospheric surface-layer turbulence, J. Fluid Mech. 273 (1994) 141. doi:10.1017/S0022112094001886.

[44] J.C. Kaimal, J.C. Wyngaard, Y. Izumi, O.R. Coté, Spectral characteristics of surface-layer turbulence, Q. J. R. Meteorol. Soc. 98 (1972) 563–589. doi:10.1002/qj.49709841707.

[45] W.J. Pierson, L. Moskowitz, A proposed spectral form for fully developed wind seas based on the similarity theory of S. A. Kitaigorodskii, J. Geophys. Res. 69 (1964) 5181–5190. doi:10.1029/JZ069i024p05181.

[46] Det Norske Veritas, Fatigue design of offshore steel structures, Norway, 2014.

[47] J. Schijve, Fatigue Properties, in Fatigue of Structures and Materials. Dordrecht: Springer (2009) 141–169. doi:10.1007/978-1-4020-6808-9_6.

[48] V. Valamanesh, A.T. Myers, Aerodynamic Damping and Seismic Response of Horizontal Axis Wind Turbine Towers, J. Struct. Eng. 140 (2014) 4014090. doi:10.1061/(ASCE)ST.1943-541X.0001018.